Structure of the diamond (111) surface: Single-dangling-bond versus triple-dangling-bond face

A. Scholze, W. G. Schmidt,* and F. Bechstedt
Friedrich-Schiller-Universität, Institut für Festkörpertheorie und Theoretische Optik, Max-Wien-Platz 1, 07743 Jena, Germany
(Received 1 December 1995)

We present converged *first-principles* calculations for the atomic and electronic structure of diamond (111) surfaces based on density-functional theory in the local-density approximation. Single- and triple-dangling-bond surfaces with 1×1, 2×1, and $(\sqrt{3}\times\sqrt{3})R30°$ translational symmetry are studied by means of total-energy minimizations. The ground-state geometries and electronic band structures are computed. In contrast to earlier work we find the π-bonded chains to be nearly undimerized and unbuckled in the 2×1 Pandey reconstruction. Consequently, the electronic band structure exhibits no optical gap. Other structures are higher in total energy (π-bonded molecule model, relaxed truncated-bulk structure) or represent only saddle points at the Born-Oppenheimer energy surface (graphitelike surface, strongly dimerized chains). Chain and trimer reconstructions at the triple-dangling-bond C(111) surface are very close in energy and domains of different reconstructions can compete. These structures may explain recent scanning tunneling microscopy findings on films grown by chemical vapor deposition. [S0163-1829(96)04519-5]

I. INTRODUCTION

Carbon modifications and carbon-bonded materials have attracted much attention during the last decade due to their growing technological importance. Much of this interest is drawn to the low-index surfaces of diamond because of their importance in epitaxial thin-film growth, in particular by chemical vapor deposition (CVD). The C(111) surfaces are of paramount interest since they appear to provide a basis for nearly atomically smooth surface growth in homoepitaxial CVD. A wide range of both experimental and theoretical investigations have been performed, but despite these efforts the exact ground-state geometry of the diamond (111) face is far from being clear. At the clean C(111) surface 1×1, $2\times2/2\times1$, and $(\sqrt{3}\times\sqrt{3})R30°$ structures have been observed. At low temperatures the (111) surface of polished diamond crystals shows a 1×1 low-energy electron diffraction (LEED) pattern which is related to a hydrogen-covered truncated-bulk geometry.[1,2] The hydrogen desorbs upon thermal annealing at 1275 K and the surface shows a rather clear 2×2 LEED pattern, which is interpreted to result from a superposition of three 2×1 rotational domains.[3,4] However, Hamza *et al.*[3] also pointed out that the hydrogen loss from the surface is necessary but not sufficient for the formation of the $2\times1/2\times2$ structure. Angle-resolved photoemission (ARPES) measurements of Himpsel *et al.*[5] on the 2×1 reconstructed surface indicated an occupied surface band that may be explained in terms of the Pandey reconstruction model [cf. Fig. 1(a)] originally introduced for silicon.[6] Support for this model came also from dynamical LEED

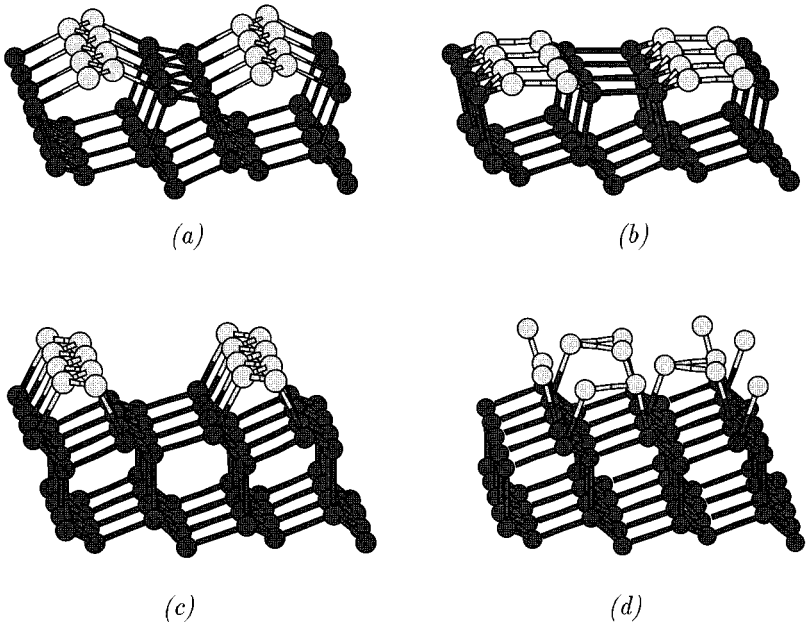

FIG. 1. Perspective views of prominent energy-minimum structures on the diamond (111) surface: (a) Pandey π-bonded chain model and (b) Chadi π-bonded molecule model at the C(111) single-dangling-bond surface; (c) the Seiwatz single-chain model; and (d) the hollow (H) site trimer model at the C(111) triple-dangling-bond surface. Carbon atoms in the uppermost surface layer are shaded.

measurements of Sowa *et al.*,[4] two-photon photoemission spectroscopy (PES) findings by Kubiak and Kolasinski[7] of an unoccupied surface band, high-resolution soft x-ray absorption measurements by Morar *et al.*,[8] and ion-scattering data.[9]

Although the Pandey chain model is now widely accepted, there remain open questions concerning the precise surface geometry, e.g., buckling or chain dimerization. The latter asymmetry has a remarkable effect on the surface electronic structure. Dimerization of the surface chain of a few percent is known to result in a significant gap opening along the *JK* line in the surface Brillouin zone (SBZ).[6] Electron-energy-loss spectroscopy (EELS) measurements as performed by Pepper[10] have been interpreted in terms of a gap of about 2.1 eV at *J*. Angle-integrated ultraviolet photoemission (UPS) and EELS measurements of Namba *et al.*[11] seem to confirm these results. However, recent work by Chin *et al.*[12] using sum-frequency generation (SFG) spectroscopy and Huisman *et al.*[13] performing grazing-incidence x-ray diffraction studies favors a buckled chain model.

So far theoretical results have also not been able to give a complete picture. First-principles calculations using a self-consistent linear combination of atomic orbitals (LCAO) approach to the density-functional theory (DFT) in the local-density approximation (LDA) by Vanderbilt and Louie[14] found undimerized π-bonded chains with a slight buckling of the surface chains of about 0.04 Å to be lowest in energy. This result is in good agreement with the tight-binding (TB) results of Chadi[15] and Bechstedt and Reichardt.[16] Other TB studies indicate a dimerization of the chains.[17] A relatively strong dimerization of 4.1% was found using a modified intermediate neglect of differential overlap (SLAB-MINDO) approach,[18] and the more recently presented local-density molecular-dynamics (LD-MD) computations of Iarlori *et al.*[19] favor chains with 1.4% dimerization. In an attempt to overcome the discrepancies between the various theoretical results, and in particular to explain the gap along the *JK* line of the SBZ, Kress *et al.*[20] presented many-body quasiparticle computations of the 2×1 surface starting from the DFT-LDA results of Ref. 14 and Ref. 19. Assuming a dimerization of 1.4% and applying quasiparticle corrections to the surface bands, a gap of about 1.7 eV occurs and the surface becomes clearly insulating in the framework of the applied perturbational theory. Nevertheless, despite these results it still remains a matter of controversial discussion whether the dimerized π-bonded chain structure provides a global minimum in total energy at the C(111)2×1 surface.

The surfaces of (111)-oriented, natural diamond samples are generally interpreted to be related to the single-dangling-bond (SDB) or shuffle-terminated faces. In a cleavage (polishing) procedure leading to such (111) faces only one bond per surface atom parallel to the surface normal has to be cut. Alternatively, triple-dangling-bond (TDB) or glide-terminated faces involve the cutting of three bonds per surface atom. The dangling bonds form an angle of 70.5° with the surface normal. This cleavage is usually rejected for energetic reasons since the cutting of three bonds needs more energy. Nevertheless, TDB cleavage has been shown to match experimental data for silicon, including the phenomenon of crack heating,[21] scanning tunneling microscopy (STM) observations,[22] or details of the surface band structure.[23] Moreover, in the case of the Si(111)2×1 surfaces cleavage modes along glide planes leading to the TDB face have already been discussed. Reichardt[24] suggested that the formation of TDB faces could be mediated by stacking faults that are generated during cleavage. The two different types of stacking faults, single or double ones, produce different surfaces, SDB or TDB faces.

In the case of diamond surfaces, hydrogen termination plays an important role. Unlike the Si(111) cleavage face, the C(111) surface exhibits a 1×1 bulklike structure after cleaving and subsequent mechanical polishing. The initial hydrogen coverage is believed to desorb after annealing.[3,4] Consequently, Zheng and Smith[18] discussed a three-step model for the chemisorption and desorption of hydrogen at the C(111) TDB cleavage face, which makes the creation of a clean TDB C(111)2×1 energetically possible. The basic idea is related to the remarkable energy gain upon the formation of C-H bonds which may compensate the energy needed to cut a C-C bond. The outstanding role of hydrogen is also obvious from the preparation of diamond films within a CVD process. $(\sqrt{3}\times\sqrt{3})R30°$ superstructures have been found by STM,[25,26] after heating up diamond (111) surfaces of polycystalline CVD films. They are related to TDB faces for symmetry reasons.

One of the first models for the Si(111)2×1 triple-dangling-bond surface has been suggested by Seiwatz.[27] It involves the formation of surface chains rather similar to the Pandey chain model in the case of the SDB face [cf. Fig. 1(c)]. Zheng and Smith[18] found this single-chain model to provide a stable energy minimum due to the strong π bonding of the undimerized chains. Theoretical investigations of the TDB C(111) surface by means of a semiempirical tight-binding molecular-dynamics (TB-MD) method[26] also give some indication for the existence of a metastable $(\sqrt{3}\times\sqrt{3})R30°$ surface geometry, which is believed to be consistent with a trimer reconstruction [cf. Fig. 1(d)]. Summarizing the results so far, the situation at the TDB surface is still a matter of speculation in spite of a few experimental measurements and theoretical calculations. However, smooth CVD-grown (111)-oriented diamond films are now available and TDB faces are very likely to exist there.

Consequently, a careful *ab initio* study of such structures in comparison with results for the SDB surface is of interest. In Sec. II an outline of the computational method is given. The results of our computations are presented in Sec. III focusing on the (111) SDB and the TDB surfaces separately. In Sec. IV a summary of the results and conclusions are given.

II. COMPUTATIONAL METHOD

We use a fully self-consistent *ab initio* pseudopotential approach to DFT (computer code FHI93CP) as described by Stumpf and Scheffler.[28] The exchange-correlation functional is treated within the LDA using the Ceperley-Alder expression[29] for the homogeneous electron gas in the parametrization of Perdew and Zunger.[30] The ion potentials are represented by fully separable, norm-conserving, *ab initio* pseudopotentials in the Kleinman-Bylander form.[31,32] The carbon pseudopotential is softened as described in Ref. 33 to ensure convergence of the ground-state properties of dia-

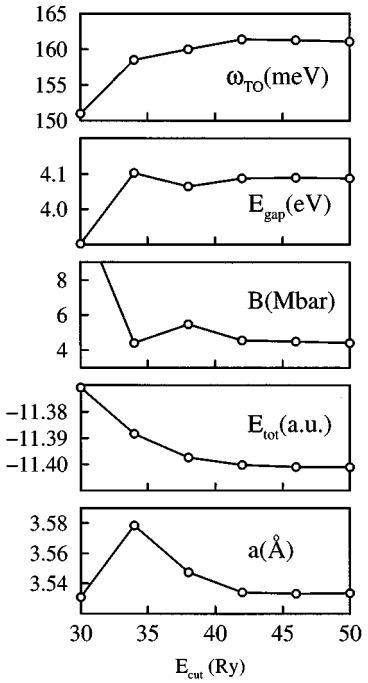

FIG. 2. Convergence of bulk diamond properties: the frequency of the transverse-optical phonon at Γ (ω_{TO}), the indirect fundamental gap (E_{gap}), the bulk modulus (B), the total energy (E_{tot}), and the equilibrium lattice constant (a) versus energy cutoff (E_{cut}).

mond for a relatively low number of plane waves in the basis set. The **k**-space integration in the SBZ is replaced by a summation over weighted special points.[34]

In order to test the softened carbon pseudopotential, a series of diamond bulk properties was calculated with different numbers of plane waves, using a sampling of two **k** points in the irreducible part of the fcc BZ.[34] Figure 2 shows that the tested bulk parameters are well converged for an energy cutoff of 42 Ry. The resulting equilibrium lattice constant amounts to 3.534 Å, being 0.9% smaller than the experimental value [3.567 Å (Ref. 35)]. The fundamental gap is 4.09 eV, some 25% smaller than the relevant experimental data [5.48 eV Ref. (35)], but in good agreement with other DFT-LDA results indicating the well-known failure of the method in calculating excited electronic states.[36] Elastic and dynamical properties such as the bulk modulus (B) and the zone-center TO phonon [$\omega_{TO}(\Gamma)$] are 4.56 Mbar [4.42 Mbar (Ref. 35)] and 161.4 meV [165.1 meV (Ref. 35)], respectively, well reproduced and in agreement with values from other DFT-LDA work such as Ref. 37.

The **k**-space summation in the SBZ is performed using sets of 16 points in the full rectangular 2×1 SBZ and six points in the full hexagonal $(\sqrt{3}\times\sqrt{3})R30°$ SBZ.[34] In case of the Pandey chain structure calculations with up to 64 points in the full SBZ were performed in order to check the sufficiency of the 16-point set. The energy minimization is based on a Car-Parrinello molecular-dynamics scheme for the self-consistent treatment of the single-particle orbitals.[38] Simultaneously, a steepest-descent approach is used to relax the atomic positions. Our energy and force calculations are converged to values within 3×10^{-4} eV and 2.5×10^{-2} eV/Å.

The SDB and the TDB surfaces are represented by symmetric slabs of 12 and 10 atomic layers, respectively, and a vacuum region equivalent in thickness. Five (four) layers on each side are relaxed. Two layers in the middle of the slab are kept bulklike. The slabs and the vacuum region between two slabs are sufficiently thick so that an almost vanishing splitting of equivalent states from opposite surfaces occurs. The plateau of the electrostatic potential in the vacuum region allows the definition of the vacuum level and is used for calculating the ionization energies.

The surface reconstruction is driven by the accompanying energy gain. The reconstruction energy is the total-energy gain upon reconstruction with respect to the ideal bulk-terminated surface, which is generally used as a reference system. It is defined per 1×1 unit cell (i.e., surface atom) as

$$E_{\mathrm{rec}}=\frac{N_s}{2n_s}(E_{\mathrm{slab}}^{\mathrm{ideal}}-E_{\mathrm{slab}}^{\mathrm{rec}}), \tag{1}$$

where N_s is the number of atoms in the slab. n_s denotes the number of atoms in the two-dimensional surface unit cell and $E_{\mathrm{slab}}^{\mathrm{rec}}$ ($E_{\mathrm{slab}}^{\mathrm{ideal}}$) is the total energy per atom of the reconstructed (ideal) slab. The energy that is needed to generate the surface reduced by the reconstruction energy E_{rec} gives the surface energy E_{sur} of the reconstructed surface, i.e., the surface creation energy,

$$E_{\mathrm{sur}}=\frac{N_s}{2n_s}(E_{\mathrm{slab}}^{\mathrm{rec}}-E_{\mathrm{bulk}}). \tag{2}$$

E_{bulk} is the total energy per atom for bulk diamond which has been calculated using a bulk supercell with $2N_s$ atoms.

On the one hand, the ionization energy I can be given as the difference between the vacuum level of the electrostatic potential and the highest occupied state in the surface electronic band structure. In metallic surface systems the Fermi level is pinned at the highest occupied state and ionization energy and work function coincide. In addition, we introduce the ionization energy I^* as the energetic distance between the vacuum level and the valence-band maximum (VBM) of the projected bulk band structure.

III. RESULTS AND DISCUSSION

A. The single-dangling-bond surface

In order to find the global minimum for the SDB C(111)2 $\times1$ surface, we considered a variety of surface configurations such as the ideal bulk-terminated surface, the relaxed truncated bulk structure, a graphitized surface,[40] the Pandey π-bonded chain model, the Chadi π-bonded molecule model, and a strongly dimerized model according to Ref. 15. Sets of atomic coordinates corresponding to these reconstruction models are taken as starting configurations in the Car-Parrinello-like energy-minimization procedure. Energetic and structural results are summarized in Table I. The unrelaxed bulk-terminated structure with zero reconstruction energy is used as an overall reference energy. The two geometries not listed in the table represent only saddle points at the Born-Oppenheimer total-energy surface. The strong dimerization in the π-bonded chains suggested by Chadi[15] decays immediately into an almost undimerized and unbuckled Pandey π-bonded chain structure. The graphitelike surface spontaneously transforms into the relaxed bulk-

TABLE I. Reconstruction energy per 1×1 unit cell, E_{rec}, surface formation energy per 1×1 unit cell, E_{sur}, and ionization energies I and I^* for stable and metastable energy-minimum structures.

Surface	Reconstruction	E_{rec} (eV)	E_{sur} (eV)	I (eV)	I^* (eV)
	Single dangling bond (SDB)				
1×1	ideal truncated bulk	0.00	3.27	5.9	6.9
1×1	relaxed truncated bulk	−0.57	2.70	4.9	6.5
2×1	Chadi π-bonded molecule	−0.73	2.54	5.3	6.2
2×1	Pandey π-bonded chain	−1.40	1.87	4.8	6.0
	Triple dangling bond (TDB)				
1×1	ideal truncated bulk	0.00	5.15	8.0	8.6
1×1	relaxed truncated bulk	−0.50	4.65	7.7	9.0
$(\sqrt{3}\times\sqrt{3})R30°$	H site trimer	−1.73	3.42	4.9	7.2
2×1	Seiwatz single chain	−1.93	3.22	6.0	6.7

terminated surface with 1×1 translational symmetry. The relaxed bulk-terminated surface, the π-bonded molecule model, and the π-bonded chain structure represent at least metastable surface structures. The largest amount of energy is released upon formation of the Pandey π-bonded chain reconstruction. The energy gain is by a factor 2 or 3 larger than in the case of the two other (meta)stable reconstructions on the SDB face.

The relaxed bulk-terminated geometry is indicated in Fig. 3(a). Although the optimization procedure is performed within a 2×1 unit cell allowing a reconstruction towards a buckling, just a simple relaxation is observed that retains the 1×1 translational symmetry. It is characterized by an inward relaxation of the first atomic layer and an outward relaxation of the second one to a value of $d_2=1.67$ Å $(+9\%)$. The energy gain upon relaxation of 0.57 eV is largely due to the shortening of the bonds between the atoms in the first and the second surface sublayer (d_1) by 4.2%. The last value is in good agreement with the results of Vanderbilt and Louie (-3.1%),[14] Stumpf and Marcus (-4.0%)[41], and a recent work by Alfonso *et al.* (-5.1%).[42] Our results confirm the conjecture of Hamza *et al.*[3] that a hydrogen-free relaxed 1×1 geometry is stable on the C(111) surface and may act as a precursor for later 2×1 reconstruction. The electronic band structure in Fig. 4(a) resembles that of the ideal bulk-terminated surface, showing two surface bands (S_1,S_2) in the 2×1 SBZ. The bands represent the folded dangling-bond band of the 1×1 SBZ because of the 1×1 translational symmetry of the surface in real space. They are degenerate along JK but remarkably split alongside ΓJ and $J'\Gamma$ due to the folding procedure. The surface is metallic and the Fermi level is pinned by partially filled bands.

The π-bonded chain reconstruction involves significant rebonding in the surface layers including the formation of surface chains with strong π bonding of the p-like dangling-bond orbitals and fivefold and sevenfold rings underneath the surface. The geometry is shown in Fig. 3(b). We find the chain bond length to be 1.43 Å, close to the mean value of

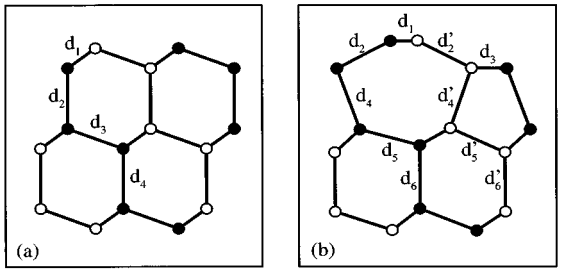

FIG. 3. Side views [atoms projected onto $(0\bar{1}1)$ plane] of the geometries of (a) the relaxed 1×1 truncated bulk structure and (b) the 2×1 π-bonded chain reconstruction.

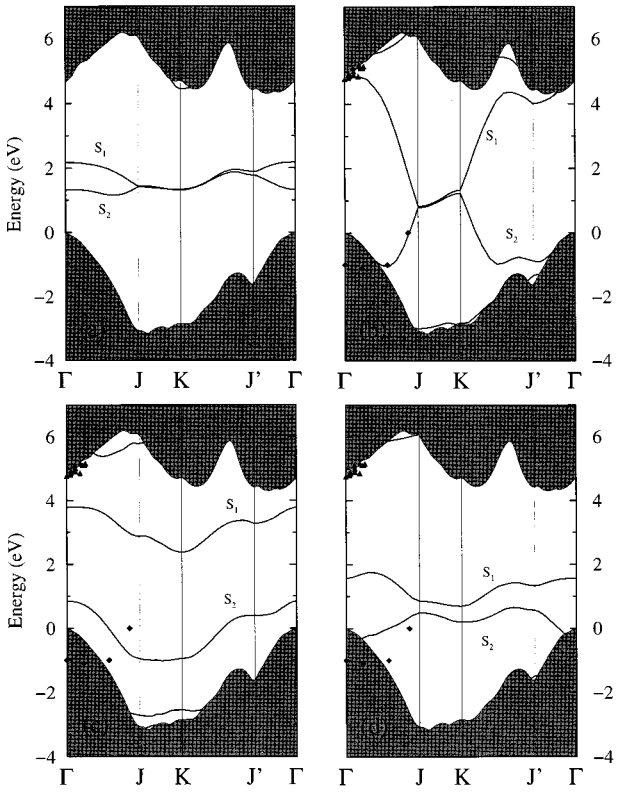

FIG. 4. Principal surface bands and projected bulk band structure (shaded) of (a) the relaxed 1×1 truncated bulk structure (shown within the 2×1 SBZ for ease of comparison), (b) the 2×1 π-bonded chain model, (c) the 2×1 π-bonded molecule surface at the single-dangling-bond surface, and (d) the 2×1 single-chain reconstruction at the triple-dangling-bond surface. Experimental data from angle-resolved PES (Ref. 5) (♦) and two-photon PES (Ref. 7) (▲) are given for comparison.

the C—C single-bond length (1.51 Å) and the C═C double-bond length (1.34 Å), thus approaching the bond length in a graphitic carbon layer (1.44 Å). This indicates that the nature of the bonding at the chain is dominated by delocalized electrons from the half filled p orbitals, similar to graphite layers or benzene molecules.

In order to find the minimum-energy structure we started from different buckled and dimerized geometries belonging to the class of the Pandey chain model. The buckling δ is given as the difference between the surface atomic coordinates in the (111) direction, perpendicular to the surface. The degree of dimerization is defined as $\Delta=(d_1-d_1')/(d_1+d_1')$ with d_1 and d_1' being the two bond lengths within the surface chain. The initial buckling and dimerization vanish very quickly after a few Car-Parrinello steps. We arrive at a rather symmetric structure with vanishing buckling of $\delta<0.01$ Å and almost no dimerization, $\Delta=0.002\%$ (16 **k** points), $\Delta=0.18\%$ (32 **k** points, 34 Ry), or $\Delta=0.3\%$ (64 **k** points, 34 Ry). The 64-**k**-point set has been proposed in Ref. 14. It is more dense in the vicinity of the zone edge of the 2×1 SBZ along the JK direction, in order to give a more accurate description of the nearly degenerate electronic bands.[39] The energy cutoff had to be reduced to 34 Ry when more than 16 **k** points were used because of computational limitations. It seems that with about 0.3% an upper limit for the dimerization can be given. Our results are in reasonable agreement with the results of Vanderbilt and Louie;[14] however, they are contradictory to those of Badziag and Verwoerd,[17] Zheng and Smith,[18] Iarlori *et al.*[19] and Alfonso *et al.*[42] They are, however, confirmed by a very recent DFT-LDA calculation using ultrasoft Vanderbilt pseudopotentials.[43]

In order to understand the trend towards inequivalent bonds in the surface chain, we performed calculations for an infinite isolated $(CH)_x$ zigzag chain. The hydrogen-saturated bonds correspond to backbonds at the C(111) surface chain. Upon relaxing this system at various lattice constants we found the energy minimum for nearly undimerized chains. The dimerization $\Delta=0.04\%$ (16 **k** points, 42 Ry) is small, but indeed one order of magnitude larger than calculated for the π-bonded chains bonded to bulk diamond. This indicates that the energy loss induced by C—C bond stretching is counterbalanced by the band structure energy gain upon dimerization. The calculated chain dimerization is smaller than measured.[44] However, real *trans*-polyacetylene chains possess a finite length in contrast to the structure considered in our work.

The Pandey chain reconstruction of the SDB surface also affects the layers below the surface. The lengths of the bonds that connect the chain to the substrate, d_2 and d_2' [cf. Fig. 3(b)], are found to be very close to the bulk bond length ($\pm0.1\%$). d_3 is stretched by 0.9%. The symmetry between the surface atoms is broken by the inequivalence of bonds between deeper layers. Especially d_4 and d_4' [cf. Fig. 3(b)] differ significantly from each other. We observe an alternating raising and lowering of the atoms causing a buckling of 0.2 Å in the fourth layer. This is accompanied by an overall weakening of the bonds d_4 and d_4' by 6.6% and 4.5%, respectively. We also observe a bond dilatation between the third and the fourth layers (d_5') of 2.6%, as well as between the fourth and the fifth layers (d_6 and d_6') of -2.8% and 4.3%, respectively.

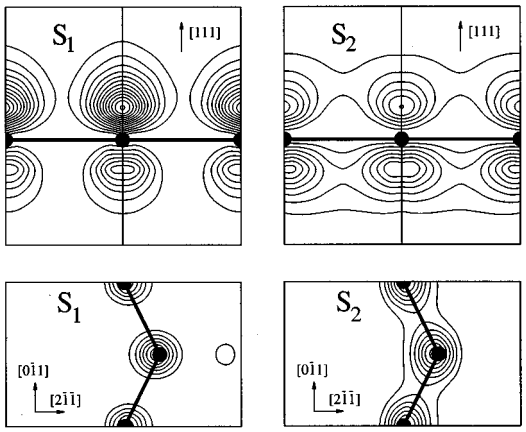

FIG. 5. Plots of the square of the wave function of the π^*-antibonding (S_1) and the π-bonding (S_2) surface states of the Pandey chain surface at the SBZ wave vector $0.4JK$. The upper panels show a projection onto the chain direction and the lower panels a top view of the surface chain. Lines of equal density are separated by 0.075 bohr^{-3}.

The electronic band structure of the relaxed C(111)2×1 Pandey chain model is shown in Fig. 4(b). The dominating features in the gap are mainly occupied (S_1) and unoccupied (S_2) surface bands derived from the π-bonding and antibonding combinations of the p orbitals along the chain and perpendicular to the surface. These surface states at the SBZ point $0.4JK$ are plotted in Fig. 5. Their π^*-antibonding and π-bonding character, the delocalized nature of the states, and the near equality of the two chain bonds within the unit cell are obvious. The one-dimensional character of the chain π bonding is clearly seen from both the surface state plots and the nearly flat and degenerate bands along JK [cf. Fig. 4(b)]. Only the small upwards dispersion of these bands and the splitting of about 0.1 eV at K results from the chain-substrate interaction. The bands cross the Fermi level and make the surface semimetallic within the DFT-LDA approach. The occupied surface state S_2 becomes resonant at half the distance ΓJ lying 1 eV below the VBM of the projected bulk band structure and shows an upwards dispersion towards J. Its dispersion seems to be in reasonable agreement with the ARPES data from Ref. 5. The splitting of S_1 and S_2 and the position of the unoccupied state at Γ with respect to the VBM at 4.8 eV are in good agreement with the findings of previous *ab initio* work,[14,19] and with the two-photon PES measurements of Kubiak and Kolasinski.[7] However, the near degeneracy of the two surface bands along JK is in contrast to the results of EELS measurements.[10] It could be lifted if the chain consisted of two chemically inequivalent atoms in the 2×1 unit cell, more strictly speaking, for dimerized chains. However, we do not find such a significant deviation from the ideal chain in our total-energy minimization. Another explanation could be related to many-body effects. Corrections to the energy eigenvalues may be obtained on the basis of a quasiparticle formalism as has been done for the C(111) surface by Kress *et al.*[20] The application of quasiparticle corrections of about 0.3 eV calculated for undimerized chains[20] does not essentially change the band structure

along JK, possibly because of the applied perturbational theory. Perhaps it is necessary to solve the full quasiparticle equations.

Besides the Pandey model there is another possibility to arrange the surface atoms in such a way that nearest neighbor interactions between half-filled p orbitals occur. The Chadi π-bonded molecule model[45] contains a strongly bound dimer molecule in the 2×1 surface unit cell. The reconstruction energy of 0.73 eV is smaller than for the π-bonded chain reconstruction. The bond length of the dimer of 1.35 Å approaches the C═C double-bond length (1.34 Å), indicating the nature of the bonding as a strong σ-π double bond. The surface electronic structure plotted in Fig. 4 shows two bands (S_1,S_2) that are associated with the π*-antibonding and π-bonding combinations of the p orbitals in the dimer, in good agreement with the LCAO band structure of Vanderbilt and Louie.[14] The position of the bands obtained is in disagreement with the PES measurements. Two backbond states associated with the fivefold and sevenfold rings between the second and the third layers, similar to those appearing in the Pandey chain model band structure, are also present in the gap region. These states are shifted more towards the center of the gap because of the stronger effect of the dimer formation on the substrate.

B. The triple-dangling-bond surface

The triple-dangling-bond face could theoretically be created upon cleaving perpendicular to the (111) direction between the two narrowly spaced layers, in contrast to the single-dangling-bond face, which separates the widely spaced bilayers at which the bonds are oriented exactly in the (111) direction. From the two possible cleavage paths the single-dangling-bond cleavage requires less energy since only one bond per atom has to be broken. The results for the surface energies clearly confirm this trend (cf. Table I). However, it is interesting to notice that although cleaving along the TDB face involves the separation of three bonds, the surface energies are not three times as large as for the SDB surface. In fact, the surface energy for the TDB minimum energy configuration is only 1.35 eV higher than for the SDB surface. Dangling bonds on the TDB face are tilted with respect to the surface normal and thus allowed to undergo considerable electronic relaxation due to next neighbor interaction between the half-filled orbitals even if the ions are kept fixed at their bulk positions. On the SDB surface there is only a very weak π-like interaction of the dangling-bond orbitals over second nearest neighbor distance.

We observe no spontaneous reconstruction of the surface if the ideal TDB surface is relaxed. The surface retains the 1×1 symmetry, only relaxing the bond lengths of the surface atoms to the substrate by -2.2%. The resulting energy gain amounts to 0.5 eV. A further lowering of the total energy may result from saturating the three dangling bonds per surface atom with hydrogen.[46] To find lower-lying energy minima of the hydrogen-free TDB surface, appropriate start geometries with symmetry breaks towards possible reconstructions have to be considered.

The earliest model that has been applied to describe the reconstruction of the TDB surface is the Seiwatz single-chain model.[27] Originally, each atom at the TDB surface is singly bonded to the second layer with three dangling bonds at each atom. The single bonds tilt to allow each surface atom to bond to two surface neighbors, leaving only one unsaturated dangling bond per atom. These dangling bonds form additional π bonds, very similar to those of the Pandey chain structure. The surface immediately acquires a 2×1 translational symmetry. The characteristic elements of the surface, the isolated (single) chains, are represented in Fig. 1(c).

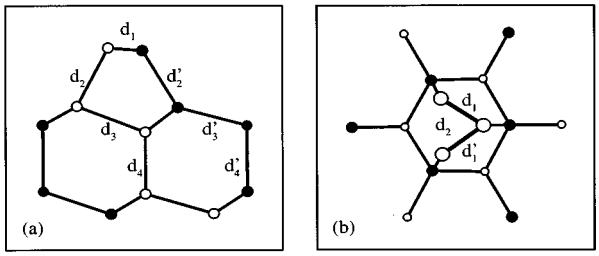

FIG. 6. Side view [atoms projected onto $(0\bar{1}\bar{1})$ plane] of the geometry of the 2×1 single-chain reconstruction on the triple-dangling-bond surface (a) and top view [atoms projected onto the (111) plane] of the $(\sqrt{3}\times\sqrt{3})R30°$ reconstruction of H site trimers on the triple-dangling-bond surface (b).

Although the overall character of the bonding is expected to be similar in both chain geometries, there are significant differences. In contrast to the Pandey reconstruction, cutting of bonds and subsequent rebonding is not necessary. The Seiwatz chain reconstruction is characterized by the formation of fivefold rings at the surface [cf. Fig. 6(a)]. The layers beneath the surface keep sixfold ring structures as in the bulk diamond structure. The sevenfold rings of the Pandey chain structure do not appear. The π bonding at the single-chain TDB surface is somewhat weaker than at the Pandey chain SDB surface. The interchain bond length d_1 is at 1.45 Å (-5.5%) slightly larger. This is due to the fact that in the Seiwatz model the p orbitals are more inclined and far from being vertical with respect to the surface normal. Moreover, the π bonding on the chain is not purely covalent. A small charge transfer accompanies a buckling of 0.05 Å between the chain atoms. The distortions caused to the other bonds in the bulk are small compared with those present in the Pandey model. At the surface sublayer only d_3' is 3.2% larger than the bulk value. d_4 and d_4' exhibit a similar relaxation (4.4%, -2.9%) as in the Pandey chain structure. All other bond lengths are within an interval of 1.2% of the bulk diamond value. The small strain in the bulk outweighs the weaker π bonds. Consequently, the reconstruction energy per surface atom of 1.93 eV is still very large, even exceeding the value for the Pandey model by 0.52 eV. Dimerization of the chain has not been found. Zheng and Smith[18] reported a five times larger buckling of 0.27 Å and a huge drop in total energy of about three times the value for their relaxed Pandey chain geometry, in sharp contrast to our results.

The electronic band structure in Fig. 4(d) is in very poor agreement with the PES data available so far for the C(111)2$\times1$ surface. The differences from the measurements in the vicinity of the Γ point are rather large at 1–2 eV. Nevertheless, some interesting features are observed. The weaker π bonding results in a narrower splitting of the π- and π*-like surface bands near Γ and J' compared to the case of

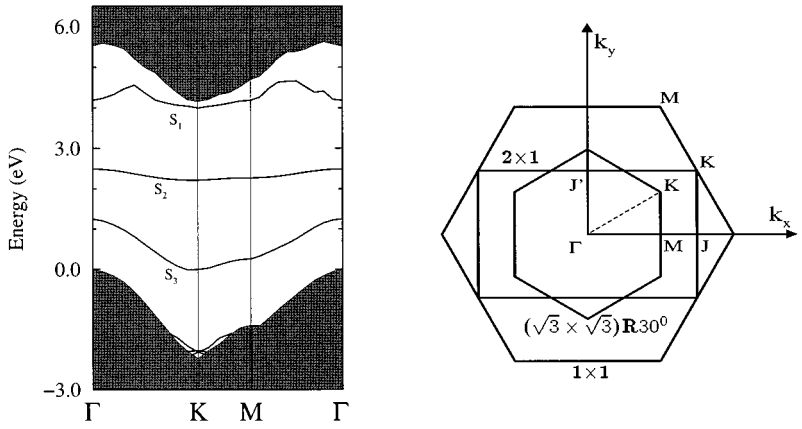

FIG. 7. Surface bands and projected bulk band structure (shaded) of the relaxed $(\sqrt{3}\times\sqrt{3})R30°$ reconstruction of H site trimers. In the right panel the SBZ of the C(111) $(\sqrt{3}\times\sqrt{3})R30°$ surface is shown in comparison with the 2×1 SBZ and the 1×1 SBZ.

the Pandey chains. The main difference from the band structure of the relaxed Pandey chain model is the appearance of a surface state gap along JK already within the DFT-LDA. It is mainly due to the slight chemical inequivalence of the chain atoms associated with the small buckling and the resulting partially ionic character of the chain bonds. The highest occupied state is located at J, whereas the lowest empty surface state occurs at K. The indirect gap amounts to only 0.04 eV. The smallest direct gap of about 0.2 eV occurs at J.

Recent STM results[25] have shown that 2×1 domains coexist with $(\sqrt{3}\times\sqrt{3})R30°$ structures. For $(\sqrt{3}\times\sqrt{3})R30°$ reconstructions of the SDB surface there exists no model that allows the half-filled dangling bonds to become nearest neighbors, hence leading to an energetically favorable reconstruction. One conceivable way is to reduce the density of dangling bonds by adsorption of one additional carbon atom per three surface atoms, still leaving one dangling bond per $(\sqrt{3}\times\sqrt{3})R30°$ unit cell. Such adatom geometries are part of the Si(111) surface reconstructions.[47] However, in contrast to the SDB surface, the TDB surface provides a natural way for the (111) surface to reconstruct by the formation of $(\sqrt{3}\times\sqrt{3})R30°$ unit cells without any additional adatoms. Consequently, it seems to be plausible that the TDB surface is a realistic basis for the explanation of the $(\sqrt{3}\times\sqrt{3})R30°$ reconstructions observed at the diamond (111) surface.

The $(\sqrt{3}\times\sqrt{3})R30°$ reconstruction observed in STM studies of polycrystalline CVD-grown films is suggested to consist of trimer structures that are centered at a hollow (H) site position on the TDB surface [cf. Fig. 1(d)]. We mention that similar reconstruction elements, such as ''milkstools''[48] and also trimers[49,50] played an important role in the first attempts to explain the structure of the Si(111)7 $\times7$ surface. The atoms forming the trimer are bonded with one bond to one carbon atom at the top substrate layer. The other three dangling bonds per atom participate in a very strong bonding within the trimer. The hollow site position is characterized by the absence of atoms centered underneath the trimer in the second substrate layer. This structure is schematically shown in Fig. 6. We relaxed the TDB surface using a trimer starting geometry which has been distorted towards the H site trimer reconstruction. The energy gain upon relaxation is 1.73 eV, only 0.19 eV lower than for the Seiwatz chain structure. From this near equality, it can be suspected that the 2×1 single-chain structure and the $(\sqrt{3}\times\sqrt{3})R30°$ H site structure compete on the TDB surface. There are observations of both translational symmetries at the same (111) facet of polycrystalline films. However, as already stated, it remains to be seen whether the 2×1 domains are reconstructed within the SDB Pandey chain or the TDB single-chain model, and, furthermore, there is no direct evidence that the $(\sqrt{3}\times\sqrt{3})R30°$ reconstruction consists of the suggested TDB H site trimer topology or rather simple adatom geometries on the SDB surface. We performed structural optimizations also for top (T) site trimers. However, these reconstruction elements are unstable.

The structural parameters of the H site trimer are rather different from the semiempirical results of Ref. 26 (values given in parentheses). The trimer forms an isosceles triangle with the equilibrium bond length of the two equally spaced bonds being $d_1=1.39$ Å (1.44 Å). The elongated bond length d_2 equals 1.52 Å (2.11 Å). The angle at the vertex of the triangle is 67° (94°). Additionally, a small downwards buckling of the associated atom of 0.1 Å is observed. The distortions on the substrate are again very small, and the reason for the large energy gain is therefore apparent. The trimer is rather symmetric, which is in agreement with the general tendency to prevent large charge transfer in the topmost layer.

The band structure of the H site trimer in Fig. 7 shows three rather flat bands in the fundamental gap of the projected bulk band structure, which are attributed to a filled S_3, a half-filled S_2, and an empty S_1 state. Plots of the corresponding wave-function squares at the K point are given in Fig. 8. These states are mainly related to π-bonding or π^*-antibonding combinations of p-like hybrids parallel to the surface normal. The σ bonds at the trimer that are parallel to the surface plane give rise to much larger splittings between bonding and antibonding states. Consequently, their bands lie in the region of the projected bulk band structure. The π character of the surface states is clearly seen from the plots of the charge densities at K (cf. Fig. 8). The S_3 state consists mainly of bonding combinations of orbitals at the vertex atom and one of the other atoms, respectively. In the S_2 case, a dangling bond appears at the vertex atom, whereas the two other dangling bonds form a bonding combination. S_1 consists only of antibonding combinations. Figure 8 also makes evident that the total charge density in the trimer region is essentially related to a

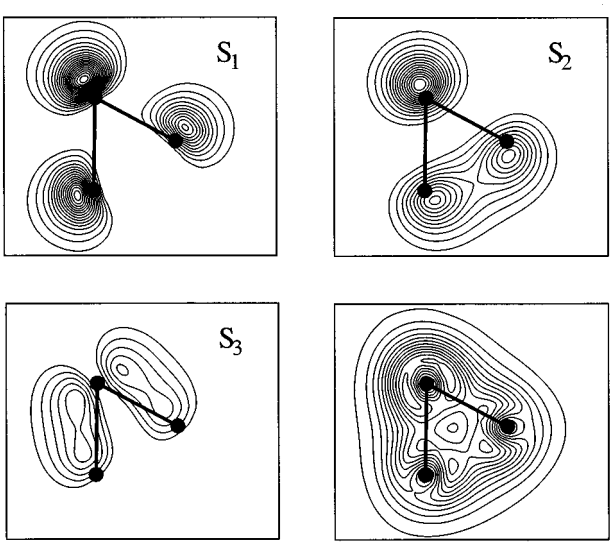

FIG. 8. Plots of the square of the wave function of the $(\sqrt{3}\times\sqrt{3})R30°$ H site trimer structure for surface bands at K. The empty S_1, the half-filled S_2, the filled surface state S_3, and the total charge density at the trimer are given in top view. Lines of equal density are separated by 0.075 bohr^{-3}.

combination of the occupied S_3 and the S_2 states. Combinations of such states may describe the observed STM images.[25]

If we compare the surface energy of the energy-minimum structure on the SDB surface, Pandey chains ($E_{\rm sur}=1.87$ eV), with the surface energy of the Seiwatz single chains ($E_{\rm sur}=3.22$ eV), which is the energy-minimum structure on the TDB surface, we can clearly conclude that the triple-dangling-bond surface is not likely to occur upon cleaving diamond bulk material. However, during CVD growth the TDB surface occurs necessarily. Because of their similar reconstruction energies, domains of 2×1 and $\sqrt{3}\times\sqrt{3}$ reconstructions may coexist.

IV. SUMMARY AND CONCLUSIONS

By means of energy- and force-minimization computations we investigated a series of reconstructions for the diamond (111) surface. We studied the TDB surface as well as the better known SDB cleavage face. The π-bonded chain model is shown to be the energy minimum structure on the single-dangling-bond cleavage surface, in overall good agreement with both experimental and earlier theoretical work. We found the TDB surface reconstructions to be characterized by even larger reconstruction energies than observed for the SDB surface. The Seiwatz single-chain structure constitutes the ground-state geometry of the TDB face. Trimer geometries are only slightly higher in energy. However, both TDB reconstructions have a higher surface energy than the Pandey π-bonded chains at the SDB surface. Nevertheless, depending upon the preparation method, TDB faces can be created. The experimental observation of a coexistence of $(\sqrt{3}\times\sqrt{3})R30°$ and 2×1 translational symmetries can naturally be explained by the small energy difference between those reconstructions at the TDB face.

ACKNOWLEDGMENTS

We acknowledge J. Furthmüller, P. Käckell, J. Pollmann, and M. Scheffler for helpful discussions. This work was supported by the Deutsche Forschungsgemeinschaft (Project No. Be1346/6-1) and the EC Program Human Capital and Mobility (Contract No. ERBCHRXCT 930 337).

*Author to whom correspondence should be addressed. FAX: +49 3641 635 182. Electronic address: W.G.Schmidt@ifto.physik.uni-jena.de.

[1] B.B. Pate, Surf. Sci. **165**, 83 (1986).
[2] B.J. Waclawski, D.T. Pierce, N. Swanson, and R.J. Celotta, J. Vac. Sci. Technol. **21**, 368 (1982).
[3] A.V. Hamza, G.D. Kubiak, and R.H. Stulen, Surf. Sci. **206**, L833 (1988).
[4] E.C. Sowa, G.D. Kubiak, R.H. Stulen, and M.A. van Hove, J. Vac. Sci. Technol. A **6**, 832 (1988).
[5] F.J. Himpsel, D.E. Eastman, P. Heimann, and J.F. van der Veen, Phys. Rev. B **24**, 7270 (1981).
[6] K.C. Pandey, Phys. Rev. B **25**, 4338 (1982).
[7] G.D. Kubiak and K.W. Kolasinski, Phys. Rev. B **39**, 1381 (1989).
[8] J.F. Morar, F.J. Himpsel, J. Hollinger, J.L. Jordon, G. Hughes, and F.R. McFeely, Phys. Rev. B **33**, 1346 (1986).
[9] T.E. Derry, L. Smit, and J.F. van der Veen, Surf. Sci. **167**, 502 (1986).
[10] S. Pepper, Surf. Sci. **123**, 47 (1982).
[11] H. Namba, M. Masuda, and H. Kuroda, Appl. Surf. Sci. **33/34**, 187 (1988).
[12] R.P. Chin, J.Y. Huang, and Y.R. Shen, Phys. Rev. B **52**, 5985 (1995).
[13] W.J. Huisman, M. Lohmeier, H.A. van der Vegt, J.F Peters, S.A. de Vries, E. Vlieg, J.F. van der Veen, T.E. Derry, and V.H. Etgens (unpublished).
[14] D. Vanderbilt and S. Louie, J. Vac. Sci. Technol. B **3**, 723 (1983); Phys. Rev. B **30**, 6118 (1984).
[15] D.J. Chadi, J. Vac. Sci. Technol. A **2**, 948 (1984).
[16] F. Bechstedt and D. Reichardt, Surf. Sci. **202**, 58 (1988).
[17] P. Badziag and W.S. Verwoerd, Surf. Sci. **194**, 535 (1988).
[18] X.M. Zheng and P.V. Smith, Surf. Sci. **253**, 395 (1991).
[19] S. Iarlori, G. Galli, F. Gygi, M. Parrinello, and E. Tosatti, Phys. Rev. Lett. **69**, 2947 (1992).
[20] C. Kress, M. Fiedler, and F. Bechstedt, Europhys. Lett. **28**, 433 (1994).
[21] Y.M. Huang, J.C.H. Spence, O.F. Sankey, and G.B. Adams, Surf. Sci. **256**, 344 (1991).
[22] Y. Mera, T. Hashizume, K. Maeda, and T. Sakurai, Ultramicroscopy **42-44**, 915 (1992).
[23] B. Chen and D. Haneman, Phys. Rev. B **51**, 4258 (1995).
[24] D. Reichardt, Prog. Surf. Sci. **35**, 63 (1991).
[25] H.G. Busmann, S. Lauer, I.V. Hertel, W. Zimmermann-Edling, H.-J. Güntherodt, Th. Frauenheim, P. Blaudeck, and D. Porezag, Surf. Sci. **295**, 340 (1993).
[26] Th. Frauenheim, U. Stephan, P. Blaudeck, D. Porezag, H.G. Busmann, W. Zimmermann-Edling, and S. Lauer, Phys. Rev. B **48**, 18 189 (1993).
[27] R. Seiwatz, Surf. Sci. **2**, 473 (1964).
[28] R. Stumpf and M. Scheffler, Comput. Phys. Commun. **79**, 447 (1994).

[29] D.M. Ceperley and B.J. Alder, Phys. Rev. Lett. **45**, 566 (1980).
[30] J.P. Perdew and A. Zunger, Phys. Rev. B **23**, 5048 (1981).
[31] L. Kleinman and D.M. Bylander, Phys. Rev. Lett. **48**, 1425 (1982).
[32] X. Gonze, R. Stumpf, and M. Scheffler, Phys. Rev. B **44**, 8503 (1991).
[33] B. Wenzien, P. Käckell, and F. Bechstedt, Surf. Sci. **307-309**, 989 (1994).
[34] D.J. Chadi and M.L. Cohen, Phys. Rev. B **8**, 5747 (1973).
[35] *Semiconductors. Physics of Group IV Elements and III-V Compounds*, edited by K.-H. Hellwege and O. Madelung, Landoldt-Börnstein, New Series, Group III, Vol. 17, Pt. a (Springer, Berlin, 1982).
[36] M. Rohlfing, P. Krüger, and J. Pollmann, Phys. Rev. B **48**, 17 791 (1993).
[37] G. Kresse, J. Furthmüller, and J. Hafner, Europhys. Lett. **32**, 729 (1995); P. Pavone, K. Karch, O. Schütt, W. Windl, D. Strauch, P. Giannozzi, and S. Baroni, Phys. Rev. B **48**, 3156 (1993).
[38] R. Car and M. Parrinello, Phys. Rev. Lett. **55**, 2471 (1985).
[39] W.G. Schmidt, A. Scholze, and F. Bechstedt, Surf. Sci. (to be published).
[40] The starting geometry for the optimization procedure contains the first two atomic layers close together and a remarkable distance of this bilayer to the third atomic layer of the ideal geometry.
[41] R. Stumpf and P.M. Marcus, Phys. Rev. B **47**, 16 016 (1993).
[42] D.R. Alfonso, D.A. Drabold, and S.E. Ulloa, Phys. Rev. B **51**, 14 669 (1995).
[43] G. Kern, J. Hafner, and G. Kresse (unpublished); G. Kern, Diploma thesis, Technische Universität Wien, 1995.
[44] C.S. Yannoni und T.C. Clarke, Phys. Rev. Lett. **51**, 1191 (1983).
[45] D.J. Chadi, Phys. Rev. B **26**, 4762 (1982).
[46] X.M. Zheng and P.V. Smith, Surf. Sci. **261**, 394 (1992).
[47] K. Takayanagi, Y. Tanishiro, M. Takahashi, and S. Takahashi, Surf. Sci. **164**, 367 (1985).
[48] L.C. Snyder, Surf. Sci. **140**, 101 (1984).
[49] F.J. Himpsel, Phys. Rev. B **27**, 120 (1983).
[50] E.G. McRae, Phys. Rev. B **28**, 2305 (1983).